

Layered Assembly of Graphene Oxide Paper for Mechanical Structures

Siyu Liu, Thomas Szkopek, Francois Barthelat, and Marta Cerruti*



Cite This: *Langmuir* 2022, 38, 8757–8765



Read Online

ACCESS |



Metrics & More

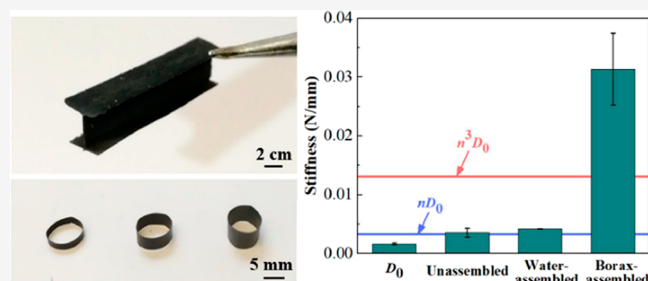


Article Recommendations



Supporting Information

ABSTRACT: Graphene oxide (GO) paper is an attractive material because of high stiffness and strength, light weight, and multiple functionalities. While these properties are now widely exploited in nanoinclusions or flat sheets, three-dimensional (3D) structures from GO paper are not widely studied because of a lack of suitable processing methods. In this study, we report a layered assembly method to make stiff and strong 3D GO structures with the aid of a sodium tetraborate (borax) solution. By comparing mechanical properties of assembled GO paper using water or borax solution, we found that the borax-assembled layers had the highest stiffness. To demonstrate the versatility of our assembly protocol, we then fabricated a variety of 3D structures including I-beams, cylindrical tubes, and bridge-like structures from GO paper. These GO structures were stiff and light weight, and the stiffness to mass ratio was around 2–4 times higher than other polymer samples including cellulose, fluorinated ethylene propylene, and poly(vinyl alcohol). The versatile processing method to make stiff and strong GO structures will enable new engineering applications where nonplanar GO structures are required.



1. INTRODUCTION

Graphene oxide (GO) has a partial sp^2 -bonded carbon structure with oxygen-containing functional groups such as hydroxyl, carboxyl, carbonyl, and epoxy groups.^{1,2} The presence of these hydrophilic groups on the hydrophobic surface of graphene gives GO an amphiphilic character.³ GO can form stable aqueous suspension that can be assembled as paper-like materials by simple solution processing methods,⁴ including directed-flow vacuum filtration,^{5–8} spin casting,⁹ spray coating,¹⁰ Langmuir–Blodgett assembly,¹¹ and self-assembly at the liquid/air interface.¹² These fabrication techniques are now well developed and finely tuned, which enables a wide range of applications for GO: bacterial inactivation and removal,¹³ wastewater treatment,^{14,15} electro-acoustic transduction,¹⁶ energy devices,^{17–20} and flexible electronics.^{21,22} These applications are however restricted to flat GO samples, and processing methods to make 3D structures would greatly extend the variety of potential applications.

Thus far, three-dimensional (3D) GO or reduced GO structures have been mainly prepared by chemical reduction with freeze-drying,²³ hydrothermal treatment,²⁴ plastic molding,^{25,26} and 3D printing by direct ink writing.^{27–31} Most of these methods introduce a porous microstructure or cannot work for pure GO, which decrease the stiffness and strength in the 3D sample. However, structures with high stiffness and strength are important in engineering applications since structures with high stiffness can resist elastic deformation and thus keep their shape and avoid unnecessary deformation

or distortion under working conditions, and structures with high strength do not easily break. Therefore, developing methods to create non-porous, high strength, and stiffness 3D GO samples is crucial for structural applications.

The 3D GO structures are expected to achieve higher mechanical properties: for example, the stiffness of an I-beam is higher than that of a flat material because of the higher second moment of area of the I-beam. However, current widely used protocols to fabricate GO paper such as vacuum filtration and drop-casting cannot be simply used for fabricating 3D structures. Additional protocols are required to fabricate 3D structures from flat GO paper.

A method proposed in the literature to build 3D GO structures takes advantage of the capability of GO flakes to restack in wet conditions: Luo et al.³² have recently demonstrated this approach by constructing 3D structures such as coils, weaves, and butterfly-shaped loops by pasting vacuum-filtered GO paper together using water. However, no mechanical tests were performed on these 3D structures; also, other water-based cross-linking solutions could be used to

Received: February 21, 2022

Revised: June 29, 2022

Published: July 14, 2022



assemble these 3D structures, which could further improve their mechanical properties.

Many cross-linkers are reported to improve mechanical properties of the GO paper, including Mg^{2+} ,³³ Ca^{2+} ,³³ Cu^{2+} ,³⁴ poly(vinyl alcohol),³⁵ polyallylamine,³⁶ polyetherimide,³⁷ 10,12-pentacosadiyn-1-ol,³⁸ borate ions,³⁹ dopamine,⁴⁰ gellan gum,⁴¹ and glutaraldehyde.⁴² These cross-linkers can interact with GO to form hydrogen or covalent bonds to produce stiffer and stronger materials, but there are no reports to date about the assembly of GO structures using a water-based cross-linking solution to improve mechanical properties.

In this study, we investigated if using a cross-linker can increase the strength and stiffness of these cut-and-paste 3D structures. We select borax (sodium tetraborate) because borax cross-linked GO paper has Young's modulus of 127 GPa,³⁹ which is, to the best of our knowledge, the highest reported value for GO paper. Borax dissolves in water forming boric acid, $B(OH)_3$, and borate ions, $B(OH)_4^-$.⁴⁴ The borate ions can react with the oxygen functional groups on GO for cross-linking.³⁹ We previously showed that borax cross-linked vacuum-filtered GO paper produced by mixing GO suspension and borax solution before filtration had greater stiffness and strength than pure GO paper.⁴³ In this study, we compare if this method of applying borax produces similarly better results when building 3D GO layered structures. Using GO paper and a borax solution, we made 3D GO structures including I-beams, cylindrical tubes, and bridge-like structures. These GO structures are stiff, strong, and light weight and outperform similar structures made with polymeric samples including cellulose, fluorinated ethylene propylene, and poly(vinyl alcohol). This study will promote the application of GO paper where stiff, strong, and lightweight 3D mechanical structures are required.

2. EXPERIMENTAL SECTION

2.1. Materials. In this study, we used a GO paste (Abalonyx Innovative Materials) that was identical to our previous reports:^{43,45} the lateral size of GO flakes was 1–25 μm (median value of 5 μm); the atomic compositions were $64.3 \pm 0.5\%$ carbon and $35.0 \pm 0.3\%$ oxygen, as measured by X-ray photoelectron spectroscopy (XPS); the relative amounts of C–C, C–O, and C=O bonds and aromatic C bonds (π – π^* shake up band) were $54 \pm 3\%$, $35 \pm 2\%$, $10.3 \pm 0.3\%$, and $0.4 \pm 0.3\%$, respectively, as calculated from C1s high-resolution XPS spectra. A borax solution (0.1 mol/L) was prepared by dissolving borax powder ($Na_2B_4O_7 \cdot 10H_2O$, Sigma-Aldrich) in water and stirring at 70 °C for 30 min. Poly(vinyl alcohol) (PVA, thickness 80 μm) membranes were prepared by drop casting a PVA solution (Sigma-Aldrich, Mw 89,000–98,000). Cellulose paper (CP, thickness of 80 μm) was acquired from Pacesetter, and fluorinated ethylene propylene (FEP, thickness of 125 μm) membranes were acquired from McMaster-Carr.

2.2. Vacuum Filtration. A GO suspension (10 mg/mL) was prepared by dissolving the GO paste in water, stirring for 30 min to exfoliate and disperse individual GO nanosheets. A controlled volume of this GO suspension was poured on the surface of a hydrophilic PVDF filter membrane (Sigma-Aldrich, GVWP09050, 90 mm diameter and 0.22 μm pore size) that was mounted on a filtration flask. The flask was connected to a vacuum pump to produce a –635 mm Hg pressure differential that forced the GO suspension through the filter. The 10, 20, 30, 80, and 200 μm -thick GO paper used in this study was prepared by using 14, 20, 26, 54, and 118 mL of GO suspension for filtration, respectively. Once the entire solution was filtered (24 h for the samples thinner than 80 μm and 48 h for the 200 μm sample), the GO paper was peeled from the filter membrane and collected for further testing and/or assembling.

2.3. Layered Assembly of Pure GO Paper. For the layered assembly of GO paper (Figure 1a), a rectangular sample (20 mm \times 2

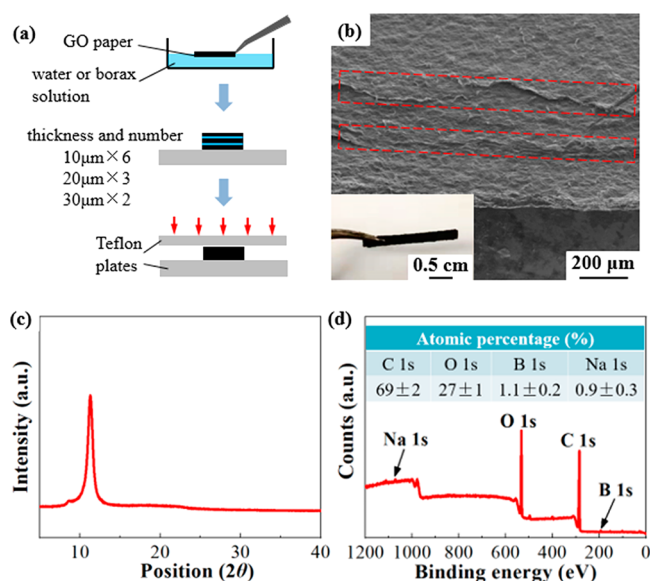


Figure 1. Layered assembly of GO paper. (a) Schematic fabrication process: first, a GO paper was placed on a Teflon plate; then, one surface of another GO paper was dipped in either water or borax solution and immediately placed on top of the first GO paper. The process was repeated several times to fabricate assembled samples with different numbers of the GO layer. Finally, the assembled sample was dried in air while pressing between Teflon plates. (b) SEM image of an assembled sample made of three 20 μm GO paper using borax solution. The dashed regions highlight the regions at the interface between different layers. A digital photograph of the assembled sample is shown in the inset. (c) XRD pattern. (d) XPS survey spectrum and elemental quantification table of the layered GO paper.

mm) was placed on a Teflon plate, and then, one side of another sample was immersed in either water or borax solution (0.1 mol/L) and attached to the previous one immediately. To study the influence of layer thickness and number of layers, three types of multi-layered samples were constructed for mechanical tests: six 10 μm -thick samples, three 20 μm -thick samples, and two 30 μm -thick samples. The GO paper was lifted by tweezers, and one side of the GO paper was brought into contact with the surface of water or borax solution (0.1 mol/L) for around 2 s. The 10 μm -thick GO paper became soft and was not able to be lifted by tweezers if the sample was contacted with water for longer than 2 s or if the sample was fully dipped into the solution. Finally, the assembled sample was dried in air for 12 h before other tests. The concentration of the borax solution (0.1 mol/L) and the time of contact between the GO paper and the solution (around 2 s) were kept constant to ensure a similar cross-linker concentration in all samples.

2.4. Layered Assembly of Borax Cross-Linked GO Paper. A series of materials were fabricated using borax as a cross-linker during the preparation GO paper. Before filtration, a 14 mL GO suspension was mixed with 1.5, 3.5, and 6.0 mL of borax solution; the concentrations of borax solution were thus diluted from 0.1 to 0.01, 0.02, and 0.03 mol/L, respectively, to achieve different degrees of cross-linking. The borax-containing GO suspension was filtered as described in Section 2.2 that produces the cross-linked GO paper. Six samples were assembled using either water or borax solution (0.1 mol/L) using the same procedure described in Section 2.3.

2.5. Layered Assembly of 3D Mechanical Structures. Different mechanical structures were assembled using the layered assembly method. I-beams (Figure 4a) were fabricated using GO paper (20 mm \times 4 mm) with thicknesses of 30, 80, and 200 μm . The fabrication started by dipping one GO paper in the borax solution and

placing it on a Teflon plate, providing a template for the flange. Then, another sample was immediately attached vertically to the horizontal piece and dried in air for 12 h to produce the web of the I-beam section. Upon drying, another GO paper was dipped to attach it to the other side of the web to produce the second flange. A holding structure (two pieces of sponge) was used to support the I-beam to ensure orthogonal joints, and the whole I-beam was finally dried for another 12 h. The density of the GO I-beam was calculated from the ratio of sample mass to volume. The mass of the sample was measured by a high-resolution balance scale (Mettler Toledo). The thickness of GO paper was measured by a micrometer before being assembled as an I-beam, and the volume was calculated from the product of sample length, width, and thickness. Cylindrical tubes (Figure 5a) were fabricated using 30 mm × 2 mm, 30 mm × 4 mm, and 30 mm × 6 mm GO paper (thickness 20 μm). The sample was manually rolled into a cylinder and was supported with a sleeve from the outside. The borax solution was poured over the overlap region of the roll to fuse the sheets, and the sample was peeled from the sleeve after 12 h of drying. Miniature bridge-like structures were fabricated by multiple GO layers with bridge profiles using the layered assembly method with the borax solution, effectively realizing a lamination assembly process. The filtered GO paper (thickness of 80 μm) was cut into three different bridge-like profile shapes, and then, 15 layers were assembled using the borax solution to produce 3D structures (the same procedure in Section 2.3). The assembled structures were finally dried in air for 12 h. All the rectangular GO paper and bridge-like samples were cut by a laser (Model Vitrolux, Vitro Laser Solutions UG, with a power of 354.8 mW and a wavelength of 355 nm) from a large filtered GO paper. To compare mechanical properties of these GO structures with other materials, we selected three widely used engineering polymer membranes (i.e., CP, FEP, and PVA) to make 3D structures and perform mechanical tests. These polymer I-beams and cylindrical tubes were fabricated by attaching the materials with double-sided tapes (Scotch 3M).

2.6. Characterization. The cross-sectional morphology and composition were characterized using a scanning electron microscope (Hitachi S4800 field emission SEM, with an accelerating voltage of 5 kV) and an energy-dispersive X-ray spectra system (Octane super 60 mm² EDS system, with an accelerating voltage of 10 kV). The observed cross section of the GO paper was created by breaking the sample after immersion in liquid nitrogen. The junction regions of GO paper, I-beams, and cylindrical tubes were also characterized by the SEM. The surface of the assembled GO paper was imaged using an optical microscope (BX-51M, Olympus). X-ray diffraction (XRD) analysis was performed using a Bruker D8 XRD system. The spectra were recorded from 3 to 40° (2θ) using a Cu Kα radiation source. XPS spectra were collected using a Thermo Scientific monochromatic Al Kα photoelectron spectrometer.

2.7. Mechanical Tests. The samples for mechanical tests were cut from the filtered GO paper with a precision laser cutting tool to ensure high control over the sample geometry and to minimize sample damage. All the mechanical tests were performed on a miniature loading stage (Ernest F. Fullam, Inc.). The assembled GO paper was tested by three-point bending to measure the stiffness and the maximum force with a 20 g load cell and a 0.02 mm/s rate to load the sample until complete failure. Some samples were highly deformable and did not break during the test; for these samples, the test was considered complete when the sample reached the largest measurable displacement allowed by the testing fixture. The load cell for testing I-beams and cylindrical tubes was 10 lbs, and the loading rate was 0.02 mm/s. The I-beams were also tested by three-point bending until complete failure of the sample. The cylindrical tubes were tested by compression because the compression test is widely used for tube structures and can assess the resistance to buckling. The compression test was performed in the axial direction between two stiff ceramic plates until complete failure of the sample.

3. RESULTS AND DISCUSSION

3.1. Layered Assembly of GO Paper. We used vacuum-filtered GO paper for the whole study. The prepared GO paper had a stacked and lamellar microstructure observed by SEM (Supporting Information, Figure S1a). The EDS spectrum (Supporting Information, Figure S1b) detected carbon, oxygen, and sulfur elements, with atomic percentages of 61.3 ± 1.2%, 38.1 ± 1.4%, and 0.22 ± 0.04%, respectively. Figure 1b shows the SEM image of a multilayer sample made with three pieces of 20 μm-thick GO paper assembled by the borax solution. The connected regions (highlighted by the dashed boxes) show no delamination between different layers, so this process effectively assembled different layers, with compact microstructures. The optical image in the inset shows that the three layers were assembled together as one sample and not detached when they were lifted by tweezers. Figure 1c and Figure 1d show the XRD pattern and XPS survey spectrum of the GO paper, respectively. The XRD spectrum shows a sharp diffraction peak at 2θ = 11.2°, indicating an ordered structure for the material with an approximate interlayer spacing of 0.79 ± 0.01 nm. In addition, XPS confirmed the presence of boron.

Figure 2 shows the mechanical properties for both assembled and unassembled layers (i.e., several layers simply

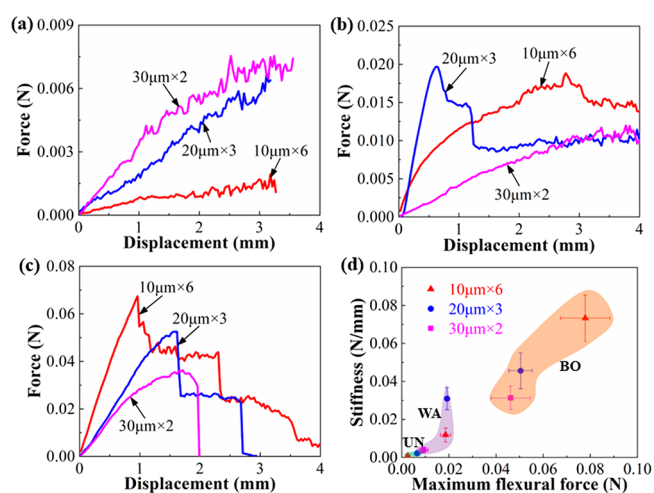


Figure 2. Three-point bending test of layered GO paper (six 10 μm-thick samples, three 20 μm-thick samples, and two 30 μm-thick samples) prepared by different methods: (a) unstacked layers; (b) assembled by water; (c) assembled by borax solution; (d) comparison of mechanical properties. UN: unstacked; WA: assembled by water; BO: assembled by borax solution.

stacked together but not dipped by any solution). Figure 2a shows the force-displacement response of the unstacked samples: the maximum force was below 10 μN, a low force which we explained by the sliding and limited interactions between different layers. The 10 μm × 6 sample had the lowest force because there were more gaps within the sample. Figure 2b shows the force-displacement curve of the water-assembled samples. The assembled samples had higher stiffness and maximum force: for example, the stiffness of the 10 μm × 6 assembled layers increased by 15.2 times, and the maximum force increased by 7.2 times, compared with the unstacked layers. Figure 2c shows the force-displacement curve of the borax-assembled samples, and Figure 2d summarizes the flexural stiffness and maximum force of all samples. Compared with the unstacked GO paper, the layered sample had

higher mechanical performance after drying because of the improved interlayer bonding caused by water or borax solution. The borax-assembled samples had higher mechanical properties than the samples assembled using water because borate ions can react with hydroxyl groups on GO to achieve cross-linking.³⁹ The 10 $\mu\text{m} \times 6$ sample had the highest stiffness, most likely because more borate ions were able to diffuse in between the GO paper for cross-linking. The stiffness of the 10 $\mu\text{m} \times 6$ sample assembled by the borax solution is 6.1 times that of the water-assembled sample. Based on the maximum flexural force (results shown in Figure 2d), we also calculated the flexural strength of the layered sample using this formula

$$\sigma_f = \frac{3FL_s}{2bh^2} \quad (1)$$

where F is the force, L_s is the span of the fixture, b is the width, and h is the thickness of the sample. Based on this calculation, the flexural strength of the 10 $\mu\text{m} \times 6$ sample layered with water was 32 ± 4 MPa, while the strength of the same sample layered with the borax solution was increased to 105 ± 14 MPa. The flexural strength of vacuum-filtered GO paper ranged between 30 and 45 MPa in our previous study.⁴³ This comparison shows that, while the flexural strength of the sample layered using water was close to that of the vacuum-filtered sample, using borax significantly improved the strength of the layered sample. Our results show that the water molecules and the borax cross-linker played key roles in this improved method: the water molecules provided a humid environment to fuse GO paper together, while the borax significantly improved the mechanical properties of the layered structures.

For the assembled layers using borax cross-linked GO paper, we found that the assembly became more difficult with an increasing amount of borax used for cross-linking: for the 0.03 mol/L borax cross-linked GO paper, the assembled samples (both dipped with water and borax solution) became delaminated immediately upon drying. The three-point bending test (Supporting Information, Figure S2) shows when using the borax cross-linked GO paper, the stiffness and maximum force were all lower than the pure GO paper assembled after dipping with borax solution (see the results in Figure 2d and Supporting Information, Figure S2c). Optical micrographs of the sample surface (Figure 3a–c) have many crystals on the borax cross-linked GO paper (0.03 mol/L) assembled after wetting with borax solution (Figure 3c). XPS spectra collected in the regions with crystals (Figure 3d) showed an evident increase in the amount of boron and sodium compared to that observed on samples that did not have such crystals (Figure 1d). The crystals also have the same rod-like shape as previously reported borax crystals,^{46,47} and since no other chemicals were used for the fabrication, it is likely that borax crystals were precipitated on the surface of GO paper. We did not observe these crystals in sample cross sections (Supporting Information, Figure S3), possibly because after dipping the GO paper in the borax solution, most solution was on the sample surface. Crystals were more likely to nucleate and grow from the sample surface where the concentration of borate ions was higher due to drying, so the borax crystals were found only on the sample surface. We did not wash the sample further because the layered sample was already delaminated, and we wanted to keep the overall steps identical for comparison. These results indicated that the GO

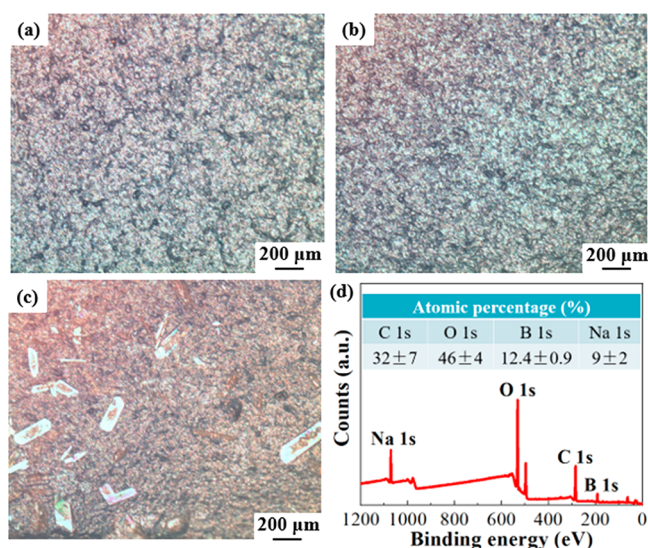


Figure 3. Surface characterization of the layered GO paper: (a) optical micrograph of pure GO paper assembled by borax solution; (b) optical micrograph of borax cross-linked GO paper (0.03 mol/L) assembled by water; (c) optical micrograph of borax cross-linked GO paper (0.03 mol/L) assembled by borax solution; (d) XPS survey spectrum of the sample in panel (c) and elemental quantification table.

paper was already saturated with borax, and no more borate ions were able to diffuse into the samples. The mechanical properties of the layered cross-linked GO paper with a lower borax concentration (0.01 and 0.02 mol/L) were lower than those achieved using the pure GO paper (Supporting Information, Figure S2). Fewer interlayer interactions were likely responsible for the lower mechanical properties of the layered borax cross-linked GO paper: since borax cross-linking occurred during filtration, most of the hydroxyl groups already reacted with borate ions and were not available for either reaction with borax or hydrogen bonding during the following layered assembly process.

In summary, of all the methods we tested, assembling the uncross-linked GO paper after dipping them with borax solution resulted in materials with the highest stiffness. For example, the stiffness of the 10 $\mu\text{m} \times 6$ sample assembled by the borax solution is 6.1 times that of the water-assembled sample. We therefore used this protocol to construct the 3D structures described in the next section.

3.2. Layered Assembly of 3D GO Structures. I-beams are widely used in structural engineering to maximize the second moment of area ($\int y^2 dA$, where A is the cross-sectional area and y is the distance from the neutral axis) so that flexural stiffness is maximized while weight is minimized. Figure 4b shows the fabricated GO I-beam by the layered assembly method, and it had nearly parallel samples (flanges) at the two sides of the central sample (web). SEM imaging of the junction of different GO paper (Figure 4c,d) shows that individual samples were completely attached, with a compact microstructure. Figure 4e shows the flexural force-displacement curves of the GO I-beams. The bending stiffness of the I-beam increased with the larger sample thickness, which is as expected due to the higher second moment of area for the thicker sample. Moreover, the thicker sample had a larger contact area between different GO paper, so more borate ions could diffuse into the thicker samples for cross-linking and contributed to

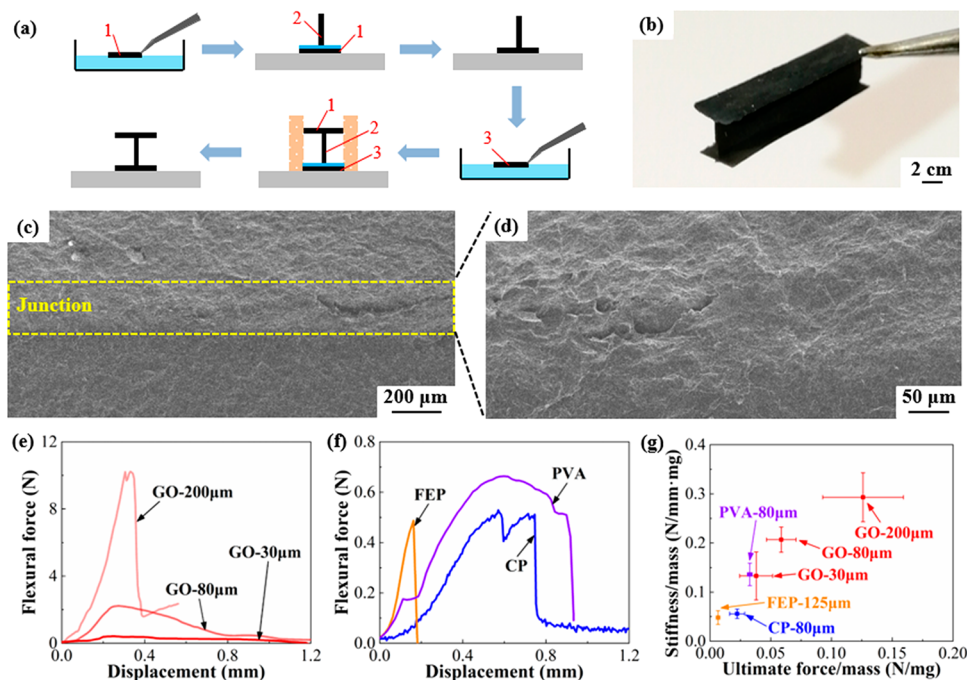


Figure 4. Fabrication and three-point bending test of I-beams. (a) Schematic fabrication process of the GO I-beam assembled by borax solution (the numbers indicate the three layers used for making the I-beam): first, the flange 1 was dipped in the borax solution and placed on a Teflon plate; then, the web 2 was vertically placed on top of the flange 1 and dried for 12 h; finally, flange 3 was dipped in the borax solution and placed onto the top side of the web 2. The whole structure was dried for another 12 h with the help of a holding structure. (b) Photograph of a GO I-beam. (c, d) SEM images of the GO I-beam at the junction with different magnifications. (e) Flexural force-displacement curve of the GO I-beam with different thicknesses (30, 80, and 200 μm). (f) Flexural force-displacement curve of I-beams pasted by CP, FEP, and PVA. (g) Comparison of stiffness to mass and ultimate force to mass ratios.

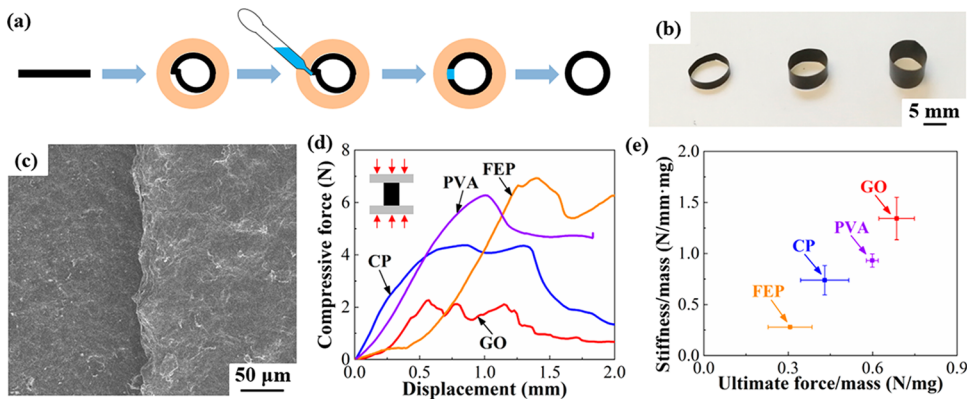


Figure 5. Fabrication and compression test of cylindrical tubes. (a) Schematic fabrication process of the GO cylindrical tube assembled by borax solution: first, the GO paper was manually rolled into a cylinder and supported with a sleeve from outside; then, the borax solution was poured over the overlap region; finally, the sample was peeled from the sleeve after 12 h of drying. (b) Photographs of GO cylindrical tubes with different heights. (c) SEM image of the GO cylindrical tube (4 mm height) at the overlap region. (d) Compressive force-displacement curve of cylindrical tubes made by GO, CP, FEP, and PVA. The schematic loading figure is shown in the inset. (e) Comparison of stiffness to mass and ultimate force to mass ratios.

the higher stiffness. The density of the 80 μm -thick GO I-beam is $1.70 \pm 0.05 \text{ g cm}^{-3}$. The value is significantly higher than freeze-dried GO aerogels, whose density has been reported to range between 0.014 and 0.081 g cm^{-3} .⁴⁸ The I-beam showed different failure modes: for the 30 and 80 μm samples, the web gradually collapsed and the load dropped slowly after reaching a peak value (Supporting Information, Figure S4a,b); for the 200 μm sample, the web remained vertical throughout the test and the failure came from the sudden breaking of the sample, with a drop of the load (Supporting Information, Figure S4c). This is mainly because a thicker web of the I-beam can prevent

distortion of the structure and thus remained vertical during the loading process and suddenly broke when the material reached its ultimate strength. This can be visualized from the photographs of the GO I-beams after the flexural tests (Supporting Information, Figure S5): neither the flanges nor the web of thin samples (80 or 30 μm) were damaged because the failure of the structure came from the detachment of different components; however, a large crack formed in the web piece of thick samples (200 μm), causing the failure of the structure. From the cross-sectional SEM image (Supporting Information, Figure S6), the fractured surface of the 200 μm

sample had a layered structure similar to that of the sample that was broken in liquid nitrogen after fracture (Supporting Information, Figure S1a). Figure 4f shows the flexural force-displacement curves of I-beams made by other polymer membranes (including CP, FEP, and PVA) for comparison. The flexural modulus of CP, FEP, and PVA were 2.1 ± 0.2 , 0.59 ± 0.05 , and 1.86 ± 0.05 GPa, respectively, from the three-point bending test (Supporting Information, Figure S7). We calculated the stiffness, ultimate force (Supporting Information, Figure S8), and the ratio of stiffness or ultimate force to mass to compare the different sample properties (Figure 4g, the mass of the polymeric samples was considered after subtracting the tape mass). As stiff and lightweight structures are desirable for many mechanical applications, we compared the overall performance of these structures by normalizing the stiffness (or ultimate force) to the sample mass. The GO I-beams had higher ratios than all other materials, which highlights that they are light weight while maintaining good mechanical properties. We were not able to use water or borax solution to attach samples made of these polymers as they were easily detached upon drying. For this reason, we used double-sided tape to make 3D structures out of these polymers. The double-sided tape created a very strong junction for these samples, as shown by the fact that, during mechanical tests, when the polymeric strips failed, the junction region was still connected (Supporting Information, Figure S9a,b). Failure of the polymeric I-beams occurred due to the sudden twisting of the web and collapse of the three pieces during loading (Supporting Information, Figure S9c).

Cylindrical tubes are another widely used type of structural elements. With a proper height, the two ends of the GO paper were able to attach to each other leading to well-sealed GO cylindrical tubes, as shown in the photographs in Figure 5b. The height of the cylinders could be changed by changing the dimension of the GO paper, up to a maximum of 6 mm (Figure 5b); beyond this value, the cylinder bent and wrinkled upon drying because of poor distribution of the borax solution in the overlap region. Figure 5c shows the SEM image of the overlap region in a 4 mm height cylinder. A shadow can be observed because of the height difference at the overlap region. Figure 5d shows the compressive force-displacement curves of cylindrical tubes made of GO, CP, FEP, and PVA with a fixed height of 4 mm. Among these materials, GO did not have the highest stiffness and ultimate force (Supporting Information, Figure S10), but when comparing the ratio of stiffness or ultimate force to sample mass, GO performed the best (Figure 5e). Cyclic loading and unloading of the GO cylindrical tubes showed that the structure was able to keep its high stiffness after 10 cycles (Supporting Information, Figure S11).

To demonstrate the versatility of the layered assembly method and the ability to create complex 3D structures, we fabricated three miniature bridge-like structures, as shown in Figure 6a–c. The assembled samples could keep their shapes and stand like miniature bridges. The GO bridges were light weight and able to hold a heavy weight (Figure 6d–f): As a demonstration, two samples of the shape shown in Figure 6b with a total weight of 0.38 g successfully supported a 200 g weight. The GO bridges delaminated and cracked if loaded with a weight of 500 g (Supporting information, Figure S12).

3.3. Discussion. In this study, we proposed a layered assembly method for GO paper using borax solution as the wetting agent instead of water³² and tested their performance on flat samples and on 3D structures that duplicate widely used

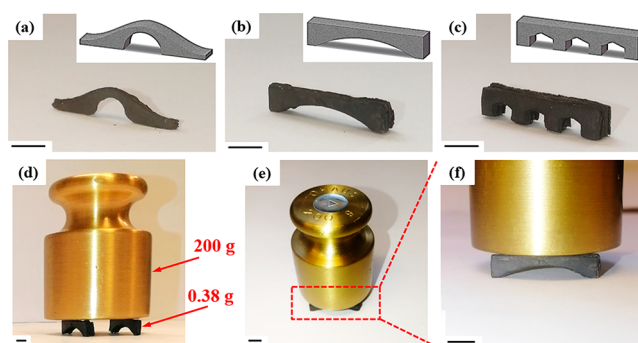


Figure 6. GO bridges assembled by borax solution. (a–c) Different bridge structures assembled by 15 pieces of 80 μm -thick GO paper. All the samples can stand vertically without any support. (d–f) Photographs showing that two pieces of the GO bridge (0.38 g in total) can hold a 200 g weight. The scale bar represents 5 mm.

mechanical elements. Our results show that, while water-assembled GO paper (Figure 2d, six layers) increased stiffness by 15-fold compared with simply stacked unassembled layers (similar to that observed by Luo et al.³²), the borax-assembled sample boosted the stiffness by 90-fold.

We now discuss a theoretical framework based on solid mechanics principles⁴⁹ to assess our mechanical results for these multi-layered GO samples. For a laminated structure that consists of n non-interacting layers of linear, elastic, homogeneous, and isotropic materials, the total bending stiffness D_n is

$$D_n = nD_0 \quad (2)$$

where D_0 is the bending stiffness of a single layer. For a bulk structure with the same total thickness, the bending stiffness becomes

$$D_n = n^3D_0 \quad (3)$$

Therefore, improving interlayer bonding can significantly improve the overall stiffness; we achieved this by attaching GO using water and borax solutions. After measuring the flexural stiffness of a 30 μm -thick GO sample, we calculated the bending stiffness of two layers without interactions (eq 2) and a bulk structure (eq 3). By comparing these theoretical values with the experimental results, we found that while the stiffness of the unassembled samples matches the theoretical value for non-interacting layers, the stiffness of the borax-assembled sample is also higher than the calculated bulk pure GO structure (Figure 7). The calculation in eq 3 does not include chemical reactions, so the higher experimental result may be due to the chemical cross-linking with borax. This is schematically shown in Figure 8. At the connection region between different GO paper, borate ions were able to react with oxygen groups on GO for cross-linking, which contributed to the enhancement of mechanical properties of 3D structures. Similar to a classical shear-tension model developed by Jager and Fratzl,⁵⁰ when the 3D GO structures were subjected to external force, the GO nanosheets carried high tensile stresses, while the borax cross-link between GO nanosheets carried shear stresses.

The average size of the GO nanosheets is also an important factor that influences the mechanical properties of the assembled macroscopic GO paper. Lin et al.⁵¹ reported that GO paper made from larger GO nanosheets has higher Young's modulus and ultimate strength because of closer-

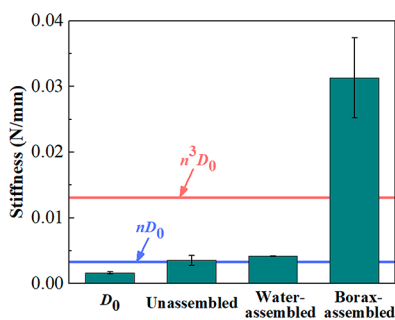


Figure 7. Stiffness comparison of the two 30 μm -thick GO paper assembled with different methods. The D_0 value is the flexural stiffness of a 30 μm -thick GO paper tested by three-point bending, and the two lines are the results calculated based on two non-interacting layers or a bulk structure, as per eqs 2 and 3, respectively. The other experimental results (unassembled, water-assembled, and borax-assembled) are the same, as shown in Figure 2d, reproduced here to facilitate the comparison.

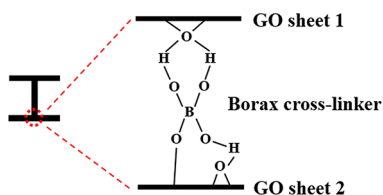


Figure 8. Schematic showing cross-linking between different GO sheets that is responsible for the mechanical performance enhancement of 3D GO structures using borax cross-linking.

stacked structures and better alignment. Therefore, we expect that the mechanical properties of assembled 3D GO structures will be enhanced further if we use GO paper filtered from larger-sized GO nanosheets.

Previous reports showed that 3D structures made with GO paper used an origami folding method^{52,53} and an embossing method,⁴⁵ but since the pure GO paper is brittle, these methods only worked for GO composite samples such as GO-cellulose^{45,52} and GO-poly(acrylic acid-co-(4-acrylamidophenyl)boronic acid).⁵³ Another widely used method to create 3D GO structures in the literature is by 3D printing with direct ink writing.^{27–31} This is an extrusion-based additive manufacturing method where a GO ink is dispensed out of small nozzles to make 3D structures. However, the structures made by 3D printing are very porous (most reports call them aerogels), which leads to lower stiffness and strength than the structures made by compact GO paper. The layered assembly method first introduced by Luo et al.³² allowed the fabrication of 3D structures with pure GO paper using water. Here, we demonstrate that stiffer and stronger mechanical structures can be assembled using borax as a cross-linker between the layers. Although borax cross-linking for GO has already been widely reported,^{39,43,44} previous works reported improved mechanical properties when GO and borax solutions were mixed before^{39,44} or during⁴³ filtration. Here, we found that the borax cross-linked GO paper did not work well for the layered assembly process because of the decreased interlayer bonding ability, whereas greater mechanical properties could be achieved by dipping pure GO paper in the borax solution to paste together different parts of the 3D structures.

GO is regarded as a functional material with interesting electrical, magnetic, or thermal properties after proper

modifications and with applications such as batteries^{17–20} and flexible electronics.^{21,22} Although the functionalization of GO is widely studied with many possible applications, the research of GO for real-life applications as a structural material is still at a preliminary stage. Most current reports discussing GO mechanical properties only showed the fundamental mechanical properties (such as Young's modulus, strength, and density) of GO paper. Fabricating 3D GO structures that mimic real-life structures and performing mechanical tests on 3D structures rather than simply on GO paper are crucial to enable the application of GO paper in load-bearing structures. In this study, we showed the possibility of using GO as a structural material to construct I-beams, cylindrical tubes, and bridge-like structures.

Our results pave the way toward using GO for manufacturing stiff, strong, and lightweight mechanical structures. Still, many challenges will need to be overcome for real-life applications of these structures and to make them competitive with other widely used structural materials (e.g., metals, alloys, and ceramics). One example is the difficulty of scaling up the manufacturing process for large structures. The samples in this study were formed by hand, and automatic methods (such as using engineering robots) will need to be developed when manufacturing large-scale samples. Another limitation for the broader applications of GO-based materials and structures is high cost. For example, the raw GO material we used in this study costs \$6 per gram, which is many times higher than commonly used engineering materials. The discovery of low-cost methods to synthesize GO will therefore be necessary to enable applications on large scales. The stability of these GO structures is also an important issue that needs to be considered. For example, the GO structures are sensitive to humidity and we found that the GO I-beam dissolved in water after 36 h with mild shaking (Supporting Information, Figure S13). The stability of GO structures in water may be improved by cross-linking with Al^{3+} ⁵⁴ or by hydrophobic coatings. The mechanical properties of GO paper also change with humidity and temperature. Hu et al.¹⁶ reported that the storage modulus of GO paper decreased from around 23 to 12 GPa when the relative humidity increased from 10% to 85% at 30 °C. The storage modulus of GO paper decreased as temperature increased from –80 °C, reaching a minimum value in the 60–70 °C range, and subsequently increased with temperature until the onset of thermal reduction.¹⁶ The stability of the 3D GO structures as a function of temperature or light irradiation should be studied in future work.

4. CONCLUSIONS

In conclusion, we reported a new protocol to achieve stiff and strong 3D GO structures where GO paper is layered using borax solution. Pure GO paper cross-linked with borax had higher stiffness and strength than simply stacked samples or using water as an interlayer wetting agent. The water-assembled GO layers (six layers) increased stiffness by 15-fold compared with simply stacked unassembled layers, while the borax-assembled sample boosted the stiffness by 90-fold. Borax-assembled GO paper could be further assembled into 3D structures including I-beams, cylindrical tubes, and bridges. These GO structures showed higher stiffness to mass and ultimate force to mass ratios than other samples made of polymer membranes including CP, FEP, and PVA. While the adoption of large-scale 3D GO structures in real-life

applications requires further work to address GO cost and difficulties in manufacturing large-scale products, the produced small-scale structures in this study demonstrate the possibility of using GO as a structural material with excellent mechanical properties.

■ ASSOCIATED CONTENT

SI Supporting Information

The Supporting Information is available free of charge at <https://pubs.acs.org/doi/10.1021/acs.langmuir.2c00442>.

Characterizations of GO paper, three-point bending test of assembled borax cross-linked GO layers and polymer membranes, photographs of the GO I-beam during the loading process, and photographs and mechanical properties of polymer 3D structures (PDF)

■ AUTHOR INFORMATION

Corresponding Author

Marta Cerruti – Department of Mining and Materials Engineering, McGill University, Montreal, QC H3A 0C5, Canada; orcid.org/0000-0001-8533-3071;
Email: marta.cerruti@mcgill.ca

Authors

Siyu Liu – Department of Mechanical Engineering, McGill University, Montreal, QC H3A 2K6, Canada; orcid.org/0000-0003-1666-3709

Thomas Szkopek – Department of Electrical and Computer Engineering, McGill University, Montreal, QC H3A 0E9, Canada; orcid.org/0000-0003-1152-6043

Francois Barthelat – Department of Mechanical Engineering, McGill University, Montreal, QC H3A 2K6, Canada; Department of Mechanical Engineering, University of Colorado, Boulder, Colorado 80309, United States; orcid.org/0000-0001-8393-3612

Complete contact information is available at: <https://pubs.acs.org/10.1021/acs.langmuir.2c00442>

Notes

The authors declare no competing financial interest.

■ ACKNOWLEDGMENTS

This study was supported by a strategic grant (STPGP 506395-17) from the Natural Sciences and Engineering Research Council of Canada. S.L. was partially supported by a McGill Engineering Doctoral Award and a B2X Doctoral Scholarship from the Fonds de recherche du Québec - Nature et technologies. S.L. would like to thank Yiwen Chen and Hao Li for the help with characterizations.

■ REFERENCES

- (1) Chen, D.; Feng, H.; Li, J. Graphene Oxide: Preparation, Functionalization, and Electrochemical Applications. *Chem. Rev.* **2012**, *112*, 6027–6053.
- (2) Kim, F.; Cote, L. J.; Huang, J. Graphene Oxide: Surface Activity and Two-Dimensional Assembly. *Adv. Mater.* **2010**, *22*, 1954–1958.
- (3) Paulista Neto, A. J.; Fileti, E. E. Elucidating the Amphiphilic Character of Graphene Oxide. *Phys. Chem. Chem. Phys.* **2018**, *20*, 9507–9515.
- (4) Pei, S.; Cheng, H. M. The Reduction of Graphene Oxide. *Carbon* **2012**, *50*, 3210–3228.
- (5) Dikin, D. A.; Stankovich, S.; Zimney, E. J.; Piner, R. D.; Dommett, G. H. B.; Evmenenko, G.; et al. Preparation and

Characterization of Graphene Oxide Paper. *Nature* **2007**, *448*, 457–460.

(6) Gong, T.; Lam, D. V.; Liu, R. L.; Won, S.; Hwangbo, Y.; Kwon, S.; Kim, J.; Sun, K.; Kim, J. H.; Lee, S. M.; Lee, C. Thickness Dependence of the Mechanical Properties of Free-Standing Graphene Oxide Papers. *Adv. Funct. Mater.* **2015**, *25*, 3756–3763.

(7) Xu, Y.; Bai, H.; Lu, G.; Li, C.; Shi, G. Flexible Graphene Films via the Filtration of Water-Soluble Noncovalent Functionalized Graphene Sheets. *J. Am. Chem. Soc.* **2008**, *18*, 5856–5867.

(8) Yang, X.; Zhu, J.; Qiu, L.; Li, D. Bioinspired Effective Prevention of Restacking in Multilayered Graphene Films: Towards the Next Generation of High-Performance Supercapacitors. *Adv. Mater.* **2011**, *23*, 2833–2838.

(9) Xu, Y.; Long, G.; Huang, L.; Huang, Y.; Wan, X.; Ma, Y. et al. Polymer Photovoltaic Devices with Transparent Graphene Electrodes Produced by Spin-Casting. *Carbon* **2010**, *11*, 3308–3311.

(10) Pham, V. H.; Cuong, T. V.; Hur, S. H.; Shin, E. W.; Kim, J. S.; Chung, J. S. et al. Fast and Simple Fabrication of a Large Transparent Chemically Converted Graphene Film by Spray-Coating. *Carbon* **2010**, *7*, 1945–1951.

(11) Li, X.; Zhang, G.; Bai, X.; Sun, X.; Wang, X.; Wang, E.; et al. Highly Conducting Graphene Sheets and Langmuir-Blodgett Films. *Nat. Nanotechnol.* **2008**, *9*, 538–542.

(12) Chen, C.; Yang, Q.; Yang, Y.; Lv, W.; Wen, Y.; Hou, P.; Wang, M.; Cheng, H. M. Self-Assembled Free-Standing Graphite Oxide Membrane. *Adv. Mater.* **2009**, *21*, 3007–3011.

(13) Musico, Y. L. F.; Santos, C. M.; Dalida, M. L. P.; Rodrigues, D. F. Surface Modification of Membrane Filters Using Graphene and Graphene Oxide-Based Nanomaterials for Bacterial Inactivation and Removal. *ACS Sustainable Chem. Eng.* **2014**, *2*, 1559–1565.

(14) Li, D.; Huang, J.; Huang, L.; Tan, S.; Liu, T. High-Performance Three-Dimensional Aerogel Based on Hydrothermal Pomelo Peel and Reduced Graphene Oxide as an Efficient Adsorbent for Water/Oil Separation. *Langmuir* **2021**, *37*, 1521–1530.

(15) Lee, J.; Chae, H.; Won, Y. J.; Lee, K.; Lee, C. H.; Lee, H. H.; Kim, I. C.; Lee, J. M. Graphene Oxide Nanoplatelets Composite Membrane with Hydrophilic and Antifouling Properties for Wastewater Treatment. *J. Membr. Sci.* **2013**, *448*, 223–230.

(16) Hu, K.; Cardenas, W.; Huang, Y.; Wei, H.; Gaskell, R.; Martel, E.; Cerruti, M.; Szkopek, T. Viscoelastic Response of Graphene Oxide-Based Membranes and Efficient Broadband Sound Transduction. *Adv. Funct. Mater.* **2022**, *32*, 2107167.

(17) Gao, W.; Wu, G.; Janicke, M. T.; Cullen, D. A.; Mukundan, R.; Baldwin, J. K.; et al. Ozonated Graphene Oxide Film as a Proton-Exchange Membrane. *Am. Ethnol.* **2014**, *53*, 3588–3593.

(18) Wu, Q.; Yu, R.; Zhou, Z.; Liu, H.; Jiang, R. Encapsulation of a Core-Shell Porous Fe₃O₄@Carbon Material with Reduced Graphene Oxide for Li⁺ Battery Anodes with Long Cyclability. *Langmuir* **2021**, *37*, 785–792.

(19) Wang, Y.; Wang, Y.; Lu, L.; Zhang, B.; Wang, C.; He, B. et al. Hierarchically Hollow and Porous NiO/NiCo₂O₄ Nanoprisms Encapsulated in Graphene Oxide for Lithium Storage. *Langmuir* **2020**, *36*, 9668–9674.

(20) Wee, B.; Hong, J. Multilayered Poly(p-phenylenevinylene)/Reduced Graphene Oxide Film: An Efficient Organic Current Collector in an All-Plastic Supercapacitor. *Langmuir* **2014**, *30*, 5267–5275.

(21) He, Q.; Wu, S.; Gao, S.; Cao, X.; Yin, Z.; Li, H.; et al. Transparent, Flexible, All-Reduced Graphene Oxide Thin Film Transistors. *ACS Nano* **2011**, *5*, 5038–5044.

(22) Su, Y.; Zhang, W.; Lan, J.; Sui, G.; Zhang, H.; Yang, X. Flexible Reduced Graphene Oxide/Polyacrylonitrile Dielectric Nanocomposite Films for High-Temperature Electronics Applications. *ACS Appl. Nano Mater.* **2020**, *3*, 7005–7015.

(23) Lv, W.; Zhang, C.; Li, Z.; Yang, Q. H. Self-Assembled 3D Graphene Monolith from Solution. *J. Phys. Chem. Lett.* **2015**, *6*, 658–668.

- (24) Bi, H.; Yin, K.; Xie, X.; Zhou, Y.; Wan, N.; Xu, F.; et al. Low Temperature Casting of Graphene with High Compressive Strength. *Adv. Mater.* **2012**, *24*, 5124–5129.
- (25) Li, Z.; Guo, F.; Pang, K.; Lin, J.; Gao, Q.; Chen, Y. et al. Precise Thermoplastic Processing of Graphene Oxide Layered Solid by Polymer Intercalation. *Nano-Micro Lett.* **2022**, *47*, 12.
- (26) Guo, F.; Wang, Y.; Jiang, Y.; Li, Z.; Xu, Z.; Zhao, X.; et al. Hydroplastic Micromolding of 2D Sheets. *Adv. Mater.* **2021**, *33*, 2008116.
- (27) Zhang, Q.; Zhang, F.; Medarametla, S. P.; Li, H.; Zhou, C.; Lin, D. 3D Printing of Graphene Aerogels. *Small* **2016**, *12*, 1702–1708.
- (28) Jiang, Y.; Xu, Z.; Huang, T.; Liu, Y.; Guo, F.; Xi, J.; et al. Direct 3D printing of Ultralight Graphene Oxide Aerogel Microlattices. *Adv. Funct. Mater.* **2018**, *28*, 1707024.
- (29) Fu, K.; Wang, Y.; Yan, C.; Yao, Y.; Chen, Y.; Dai, J.; et al. Graphene Oxide-Based Electrode Inks for 3D-Printed Lithium-Ion Batteries. *Adv. Mater.* **2016**, *28*, 2587–2594.
- (30) Zhu, C.; Han, T. Y.; Duoss, E. B.; Golobic, A. M.; Kuntz, J. D.; Spadaccini, C. M.; Worsley, M. A. Highly Compressible 3D Periodic Graphene Aerogel Microlattices. *Nat. Commun.* **2015**, *6*, 6962.
- (31) García-Tuñón, E.; Barg, S.; Franco, J.; Bell, R.; Eslava, S.; D'Elia, E.; et al. Printing in Three Dimensions with Graphene. *Adv. Mater.* **2015**, *27*, 1688–1693.
- (32) Luo, C.; Yeh, C. N.; Baltazar, J. L.; Tsai, C. L.; Huang, J. A Cut-And-Paste Approach to 3D Graphene-Oxide-Based Architectures. *Adv. Mater.* **2018**, *30*, 1706229.
- (33) Park, S.; Lee, K. S.; Bozoklu, G.; Cai, W.; Nguyen, S. T.; Ruoff, R. S. Graphene Oxide Papers Modified by Divalent Ions-Enhancing Mechanical Properties via Chemical Cross-Linking. *ACS Nano* **2008**, *2*, 572–578.
- (34) Wang, Y.; Mei, Y.; Huang, F.; Yang, X.; Li, Y.; Li, J.; et al. Ultra-Robust and High-Toughness Graphene Oxide Papers via Synergistic Strengthening by Addition of Carbon-Nanotubes and Copper Ions. *Carbon* **2019**, *147*, 490–500.
- (35) Putz, K. W.; Compton, O. C.; Palmeri, M. J.; Nguyen, S. T.; Brinson, L. C. High-Nanofiller-Content Graphene Oxide-Polymer Nanocomposites via Vacuum-Assisted Self-Assembly. *Adv. Funct. Mater.* **2010**, *20*, 3322–3329.
- (36) Park, S.; Dikin, D. A.; Nguyen, S. T.; Ruoff, R. S. Graphene Oxide Sheets Chemically Cross-Linked by Polyallylamine. *J. Phys. Chem. C* **2009**, *113*, 15801–15804.
- (37) Tian, Y.; Cao, Y.; Wang, Y.; Wang, W.; Feng, J. Realizing Ultrahigh Modulus and High Strength of Macroscopic Graphene Oxide Papers Through Crosslinking of Mussel-Inspired Polymers. *Adv. Mater.* **2013**, *25*, 2980–2983.
- (38) Cheng, Q.; Wu, M.; Li, M.; Jiang, L.; Tang, Z. Ultratough Artificial Nacre Based on Conjugated Cross-Linked Graphene Oxide. *Am. Ethnol.* **2013**, *52*, 3750–3755.
- (39) An, Z.; Compton, O. C.; Putz, K. W.; Brinson, L. C.; Nguyen, S. T. Bio-Inspired Borate Cross-Linking in Ultra-Stiff Graphene Oxide Thin Films. *Adv. Mater.* **2011**, *23*, 3842–2846.
- (40) Cui, W.; Li, M.; Liu, J.; Wang, B.; Zhang, C.; Jiang, L.; et al. A Strong Integrated Strength and Toughness Artificial Nacre Based on Dopamine Cross-Linked Graphene Oxide. *ACS Nano* **2014**, *8*, 9511–9517.
- (41) Kang, D.; Cai, Z.; Jin, Q.; Zhang, H. Bio-Inspired Composite Films with Integrative Properties Based on the Self-Assembly of Gellan Gum-Graphene Oxide Crosslinked Nanohybrid Building Blocks. *Carbon* **2015**, *91*, 445–457.
- (42) Gao, Y.; Liu, L. Q.; Zu, S. Z.; Peng, K.; Zhou, D.; Han, B. H.; et al. The Effect of Interlayer Adhesion on the Mechanical Behaviors of Macroscopic Graphene Oxide Papers. *ACS Nano* **2011**, *5*, 2134–2141.
- (43) Liu, S.; Hu, K.; Cerruti, M.; Barthelat, F. Ultra-Stiff Graphene Oxide Paper Prepared by Directed-Flow Vacuum Filtration. *Carbon* **2020**, *158*, 426–434.
- (44) Lai, C.; Chen, J.; Fu, Y.; Liu, W.; Zhong, Y.; Huang, S.; Hung, W. S.; Lue, S. J.; Hu, C. C.; Lee, K. R. Bio-Inspired Cross-Linking with Borate for Enhancing Gas-Barrier Properties of Poly(vinyl alcohol)/Graphene Oxide Composite Films. *Carbon* **2015**, *82*, 513–522.
- (45) Liu, S.; Cerruti, M.; Barthelat, F. Plastic Forming of Graphene Oxide Membranes into 3D Structures. *ACS Nano* **2020**, *14*, 15936–15943.
- (46) Garrett, D.; Rosenbaum, G. Crystallization of Borax. *Ind. Eng. Chem. Res.* **1958**, *50*, 1681–1684.
- (47) Randolph, A. D.; Puri, A. D. Effect of Chemical Modifiers on Borax Crystal Growth, Nucleation and Habit. *AIChE J.* **1981**, *27*, 92–99.
- (48) Sui, Z. Y.; Han, B. H. Effect of Surface Chemistry and Textural Properties on Carbon Dioxide Uptake in Hydrothermally Reduced Graphene Oxide. *Carbon* **2015**, *82*, 590–598.
- (49) Wang, B.; Li, Z.; Wang, C.; Signetti, S.; Cuning, B. V.; Wu, X.; et al. Folding Large Graphene-on-Polymer Films Yields Laminated Composites with Enhanced Mechanical Performance. *Adv. Mater.* **2018**, *30*, 1707449.
- (50) Jager, I.; Fratzl, P. Mineralized Collagen Fibrils: A Mechanical Model with a Staggered Arrangement of Mineral Particles. *Biophys. J.* **2000**, *79*, 1737–1746.
- (51) Lin, X.; Shen, X.; Zheng, Q.; Yousefi, N.; Ye, L.; Mai, Y. W.; et al. Fabrication of Highly-Aligned, Conductive, and Strong Graphene Papers Using Ultralarge Graphene Oxide Sheets. *ACS Nano* **2012**, *6*, 10708–10719.
- (52) Liu, L.; Niu, Z.; Zhang, L.; Zhou, W.; Chen, X.; Xie, S. Nanostructured Graphene Composite Papers for Highly Flexible and Foldable Supercapacitors. *Adv. Mater.* **2014**, *26*, 4855–4862.
- (53) Zhang, M.; Huang, L.; Chen, J.; Li, C.; Shi, G. Ultratough, Ultrastrong, and Highly Conductive Graphene Films with Arbitrary Sizes. *Adv. Mater.* **2014**, *26*, 7588–7592.
- (54) Yeh, C.; Raidongia, K.; Shao, J.; Yang, Q.; Huang, J. On The Origin of The Stability of Graphene Oxide Membranes in Water. *Nat. Chem.* **2015**, *5*, 166–170.

Recommended by ACS

Electrospraying Graphene Nanosheets on Polyvinyl Alcohol Nanofibers for Efficient Thermal Management Materials

Jinghao Huo, Shouwu Guo, et al.

APRIL 04, 2023

ACS APPLIED NANO MATERIALS

READ 

Mechanically Stable Ultrathin Layered Graphene Nanocomposites Alleviate Residual Interfacial Stresses: Implications for Nanoelectromechanical Systems

Maxime Vassaux, Peter V. Coveney, et al.

DECEMBER 14, 2022

ACS APPLIED NANO MATERIALS

READ 

Graphene Interlocking Carbon Nanotubes for High-Strength and High-Conductivity Fibers

Lijun Li, Jin Zhang, et al.

JANUARY 20, 2023

ACS APPLIED MATERIALS & INTERFACES

READ 

Maintaining Colloidal Stability of Polymer/Reduced Graphene Oxide Nanocomposite Aqueous Dispersions Produced via *In Situ* Reduction of Graphene Oxide for th...

Namrata Maslekar, Vipul Agarwal, et al.

MARCH 16, 2023

ACS APPLIED NANO MATERIALS

READ 

Get More Suggestions >